UMYU Scientifica, Vol. 3 NO. 3, September 2024, Pp 239 – 250
https://doi.org/10.56919/usci.2433.027
ISSN: 2955 – 1145 (print); 2955 – 1153 (online)
A periodical of the Faculty of Natural and Applied Sciences, UMYU, Katsina

ORIGINAL RESEARCH ARTICLE

The Folding Potential of Elastically Scattered d+ ^{24}Mg Employing B3Y-Fetal Interaction within the Double Folding Model Framework

Raymond C. Abenga[1], Yahaya Y. Ibrahim[2] and Idris D. Adamu[2]
[1]Department of Pure and Applied Physics, Veritas University Abuja, Nigeria
[2]Department of Physics, Bayero University Kano, Nigeria

ARTICLE HISTORY
Received June 02, 2024
Accepted September 10, 2024
Published September 16, 2024

KEYWORDS
B3Y-Fetal, Cross-Section, Double-folding, Elastic Channel, Folding potential

ABSTRACT
The analysis of the deuteron scattering from ^{24}Mg was performed in the elastic channel using the double-folding model to evaluate the optical potentials of the present study. Both the real and the imaginary parts of the optical potentials were computed using a mass-dependent interaction (B3Y-Fetal) in the double-folding formalism. The derived double-folding potentials were used to analyse the differential cross-sections of d + ^{24}Mg within the energy range of 60-170 MeV. With the derived optical potentials, the reaction and differential cross-sections of d + ^{24}Mg were extracted in the optical model. The plots of the computed differential cross-sections were made and the results were compared to those obtained experimentally to ascertain the suitability of the derived potentials and the B3Y-Fetal interaction. In conclusion, the optical potentials obtained using the double-folding model with the B3Y-Fetal interaction were successful in reproducing the experimental data.

INTRODUCTION

In recent years, nuclear physicists have paid a great deal of attention to the topic of developing the most appropriate type of nuclear potential to study nuclear interactions (Kurkcuoglu et al., 2006). Over the years, several theoretical models that explain nuclear interactions and the structure of the interacting nuclei have been developed to compute nuclear potential (Ibraheem et al., 2023). The application of computational techniques in determining nuclear optical potentials has resulted in unprecedented success. To this end, phenomenological and folding potentials were developed and widely used in nuclear structure and reaction studies (Amer et al., 2016).

Over the years, the densities of the interacting nuclei have been linked with actual nucleon-nucleon (NN) interactions within the framework of the folding model (FM) to provide a good description of the nuclear optical potentials (Farid et al., 2001). The ability to employ folding potentials to give a coherent description of interacting systems makes them interesting. The phenomenological potentials' complexity is decreased with folding potentials (Farid, 2002). The target and arriving nuclei's density distributions are integrated with an effective nucleon-nucleon interaction to compute the folding potentials (Hagino et al., 2006).

The optical potentials derived from the folding models are considered suitable due to their ease of manipulation and the ability of the folding formalism to provide a comprehensive description of the interacting system. By utilising a phenomenological approach, the complex optical potential's imaginary component is considered, allowing for microscopic analysis of the folded potentials while taking into consideration the effects of absorption. The application of folding potentials in the analysis of scattering data in the elastic channel for nuclear reaction investigations has garnered significant interest (Behairy et al., 2015; Farid et al., 2014; Satchler, 1983).

In this work, rather than using phenomenological potentials to account for the imaginary part of the optical potential, the double-folding model was used to evaluate both the real and imaginary parts of the optical potentials for the optical model analysis. The suitability of the B3Y-Fetal interaction for nuclear reaction studies was also taken into consideration. Hence, the double-folding model is employed in this study to ascertain the intricate optical potential. The objective of this work is to develop an optical potential to examine the scattering data of the

Correspondence: Raymond Chivirter Abenga. Department of Pure and Applied Physics, Veritas University Abuja, Nigeria.
✉ raymondabenga@gmail.com
How to cite: Abenga, R. C., Ibrahim, Y. Y., & Adamu, I. D. (2024). The Folding Potential of Elastically Scattered d+ ^{24}Mg Employing B3Y-Fetal Interaction within the Double Folding Model Framework. *UMYU Scientifica*, 3(3), 239 – 250. https://doi.org/10.56919/usci.2433.027

reaction between a deuteron (d) and a ^{24}Mg nucleus in the elastic channel.

THEORETICAL FRAMEWORK

Different forms of nucleon-nucleon interactions, such as the Michigan three Yukawa interaction (M3Y) interaction, have been used for the studies of nuclear matter properties (Anantaraman et al., 1983; Burtebayev et al., 2020; Kobos et al., 1982; Satchler & Love, 1979). The M3Y interactions were used to study nuclear matter properties and reactions and were quite successful. In a recent study, mass-dependent interactions dubbed the B3Y-Fetal interaction were derived. The interactions were derived using mass numbers $A = 16$, 24, 40, and 90. Although the interactions are systematically mass-dependent, it is recommended that they be used in the study of nuclear structure and reactions for all nuclei. (Fiase et al., 2002).

In this study, a mas-dependent interaction dubbed the B3Y-Fetal interaction was derived using the strengths of the isoscalar component of the central potential of Table VII (Fiase et al., 2002). The direct, $V_{00}^{D}(s)$ and exchaange, $V_{00}^{Ex}(s)$ components of the isoscalar B3Y-Fetal interaction may be expressed as (Abenga et al., 2020),

$$V_{00}^{D}(s) = 7419.23\frac{e^{-4s}}{4s} - 1823.98\frac{e^{-2.5s}}{2.5s}, \quad (1)$$

similarly, the exchange term is determined as follows:

$$V_{00}^{Ex}(s) = 4745.02\frac{e^{-4s}}{4s} - 1984.144\frac{e^{-2.5s}}{2.5s} - 7.8474\frac{e^{-0.7072s}}{0.7072s} \quad (2)$$

In order to incorporate the impact of antisymmetrization resulting from the exchange of nucleons between the projectile and target nuclei, the folding calculations include the contribution of single nucleon knock-on exchange. Research has demonstrated that the effects of knock-on exchange may be precisely calculated by using a zero-range pseudo-potential, $\mathcal{F}_{Ex}\delta(r)$, (Brandan & Satchler, 1997; Love & Owen, 1975), and the interaction for the folding calculation becomes,

$$V_{tp}(s,E) = \left[7419.23\frac{e^{-4s}}{4s} - 1823.98\frac{e^{-2.5s}}{2.5s}\right] + \mathcal{F}_{Ex}(E)\delta(s), \quad (3)$$

The inclusion of the zero-range pseudo-potential is essential to incorporate the exchange component within the effective interaction. The form of the zero-range pseudo-potential included in equation (6) is given as,

$$\mathcal{F}_{Ex} = J_{Ex}g(E) \quad (4)$$

where $g(E)$ is an energy scaling factor. According to the calculations by (Abenga et al., 2020, 2021), the exchange amplitude J_{Ex} of the B3Y-Fetal interaction has a magnitude of around -361 MeV. The energy scaling factor of the B3Y-Fetal contact was estimated to be $\left[1 - 0.005\left(\frac{E}{A}\right)\right]$, which is similar to that of the M3Y-Paris interaction (Khoa et al., 1996) in order to accommodate the energy variance.

Studies have shown that the nuclear matter properties are not reproduced by the bare NN (B3Y-Fetal) interaction alone. Therefore, a density-dependence component had to be added to the original B3Y-fetal interaction (Khoa & Von Oertzen, 1993). The primary goal of adding the density dependence factor to the bare interaction is to stabilise the nuclear matter rather than cause it to collapse at the saturation condition (Zang et al., 2007). The density-dependent component $f(\rho)$ is included into the effective interaction according to the proposition given by (Hamada et al., 2016; Moharram & El-Shal, 2002),

$$V_{00}^{DD}(s,\rho,E) = f(\rho)V_{tp}(s,E) \quad (5)$$

The explicit form of the density dependence form factor under consideration is the exponential one, and it is expressed as (Khoa et al., 1996; Khoa & Von Oertzen, 1993),

$$f(\rho) = C\left(1 + \alpha\, exp\,(-\beta\rho)\right) \quad (6)$$

where C, α, and β are constants. Equation (3) was parametrized by (Abenga et al., 2020) at the saturation state to yield the accurate value of the nuclear matter binding energy at $\in = -16$ MeV.

OPTICAL MODEL: DOUBLE-FOLDING POTENTIAL

The optical potential, $U(r)$, that was employed in this investigation was thought to be complex. The potential strengths are calculated using the double-folding model approach. In the folding formalism, the folding potential, $V_F(r)$, was computed by averaging the density-dependent B3Y-Fetal interaction and the densities of the interacting nuclei (projectile ρ_p and target ρ_t). The potential of the double-folding model is provided by (Brandan & Satchler, 1997; Satchler & Love, 1979);

$$V_F(\boldsymbol{r}) = \iint \rho_p(\boldsymbol{r_p})\rho_t(\boldsymbol{r_t})V_{pt}(\boldsymbol{s} - \boldsymbol{r_p} + \boldsymbol{r_t})d^3r_p d^3r_t, \quad (7)$$

where V_{pt} is the density-dependent B3Y-Fetal interaction defined by Equation (5).

The Fermi-type function was used in this investigation to characterise the target or incoming nuclei's nuclear and charge densities. Specifically, the two-parameter Fermi (2pF) function, which is a Fermi function with two parameters, was applied. The 2pF function is defined as (El-Attar et al., 2008),

$$\rho_{n(p)}(r) = \rho_{0n(p)}\left[1 + \exp\left(\frac{r - R_{p(n)}}{a_{p(n)}}\right)\right]^{-1} \quad (8)$$

where ρ_0, $R_{p(n)}$, and $a_{p(n)}$ are the nuclear matter density parameters.

The proton (neutron) half-density radii $R_{p(n)}$ were parameterised as (De Vries et al., 1987; Olorunfunmi & Olatinwo, 2023),

$$\left.\begin{aligned} R_p &= 0.449 + 0.0071\left(\frac{Z}{N}\right) \\ R_n &= 0.446 + 0.0072\left(\frac{N}{Z}\right) \end{aligned}\right\} \quad (9)$$

The numerical value of ρ_0 is determined from the condition that $\rho_0 = Z$ for proton and $\rho_0 = A - Z$ for neutron (De Vries et al., 1987).

The effective interaction included in Equation (7) is real, and it is expected to account for the bare potential only. The immediate consequence was that the imaginary potential, which accounts for the polarization effect, must be constructed separately. However, this work accounted for the polarization effect by including an imaginary potential using the folding approach. With this proposition, the present nuclear potential was taken in the form (Abenga et al., 2023):

$$U(r) = (N_r + iN_i)V_F(r) + V_{Coul}(r) \quad (10)$$

Here, $N_{r(i)}$ represents the potential adjustment parameters for the complex nuclear potential, whereas $V_{Coul}(r)$ denotes the Coulomb potential. The use of the renormalization parameters was to enhance the accuracy of the theoretical calculations to align with the observed data.

RESULTS

The angular distribution data of elastically scattered $\mathrm{d} + {}^{24}\mathrm{Mg}$ within the incident laboratory, energies of $60 - 170$ MeV were analysed utilising the DFM approach. The components of the complex nuclear potentials were computed employing the optical model framework outlined in Section 3. The optical potential was characterised by both the real and imaginary components, which were assumed to be equivalent but adjusted using distinct renormalization factors.

The calculated reaction (σ_r) cross-section is detailed in Table 1. In comparison to results derived from phenomenological and semi-microscopic potentials (Bäumer et al., 2001; Farid et al., 2014; Ibraheem, 2016), the current computation reveals reduced values of σ_r. The parameters of optimum fit from the folding calculations and the accompanying evaluated reaction cross-sections are shown in Table 1.

Table 1: Best-fit parameters deduced from the double folding calculations and other kinematical parameters of elastic scattering of $\mathrm{d} + {}^{24}\mathrm{Mg}$.

Target	E_{lab} (MeV)	N_r	N_i	σ_r (mb)
^{24}Mg	60.0	1.30	0.60	1048.35
	60.6	1.25	0.70	1077.21
	64.0	1.20	0.60	1021.51
	66.0	1.20	0.60	1013.40
	68.0	1.20	0.60	1005.45
	70.0	1.18	0.60	995.85
	72.0	1.20	0.60	989.99
	74.0	1.20	0.65	1002.96
	76.0	1.20	0.65	995.74
	77.3	1.20	0.65	991.11
	78.0	1.20	0.65	988.63
	80.0	1.15	0.58	947.67
	90.0	1.18	0.6	925.06
	170.0	1.20	0.75	770.26

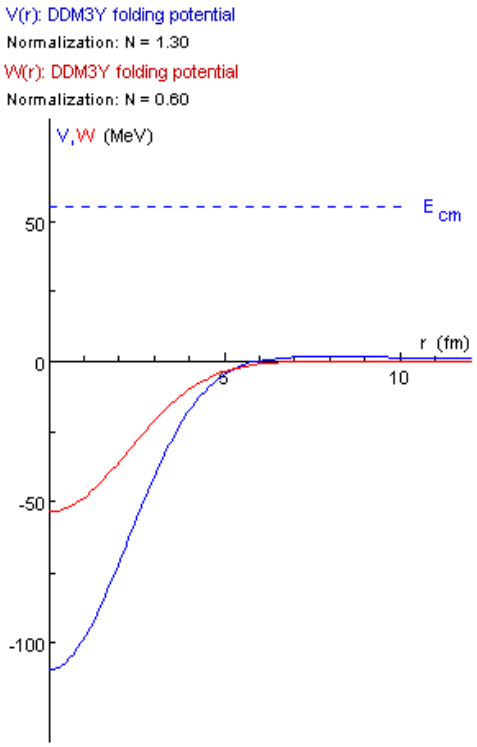

Figure 1: Optical potential of $d + {}^{24}Mg$ at $E_{lab} = 60$ MeV.

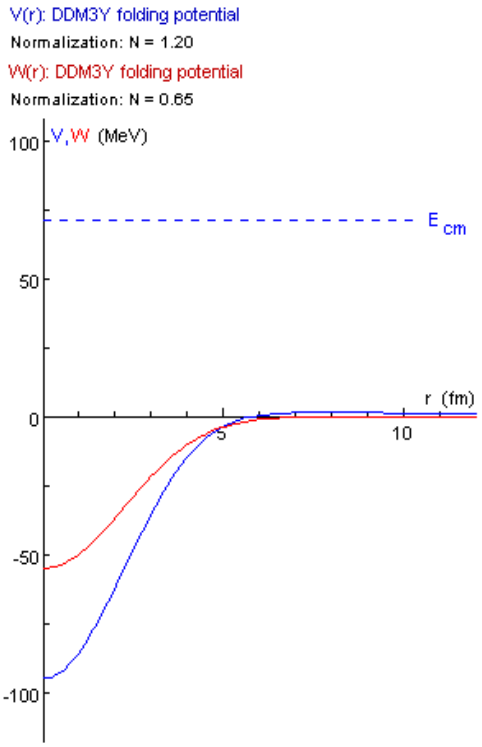

Figure 2: Optical potential of $d + {}^{24}Mg$ at $E_{lab} = 77.3$ MeV.

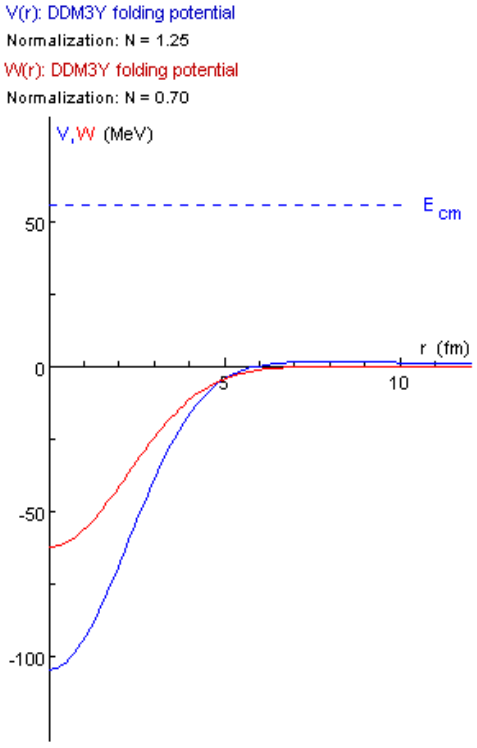

Figure 3: Optical potential of $d + {}^{24}Mg$ at $E_{lab} = 60.6$ MeV.

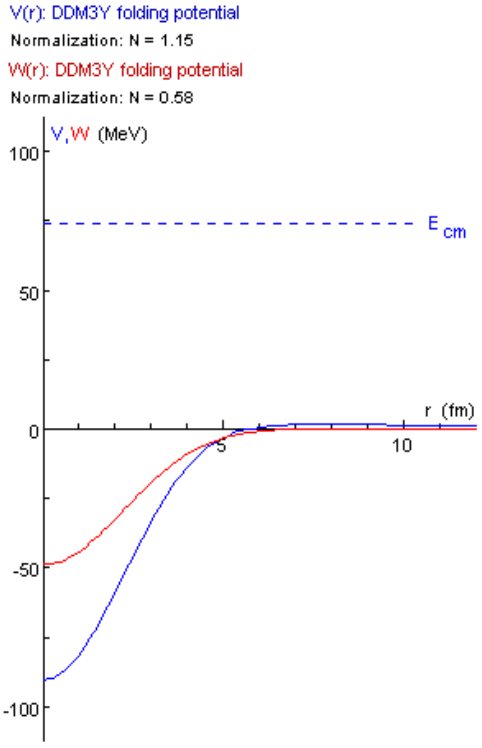

Figure 4: Optical potential of $d + {}^{24}Mg$ at $E_{lab} = 64$ MeV.

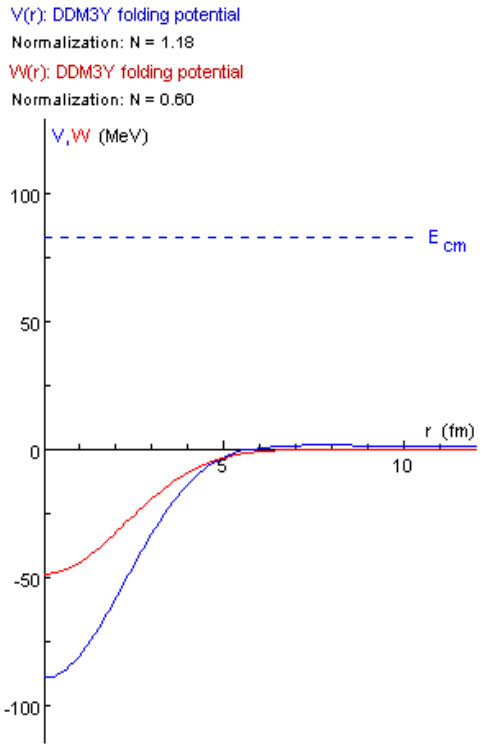

Figure 5: Optical potential of $d + {}^{24}Mg$ at $E_{lab} = 66$ MeV.

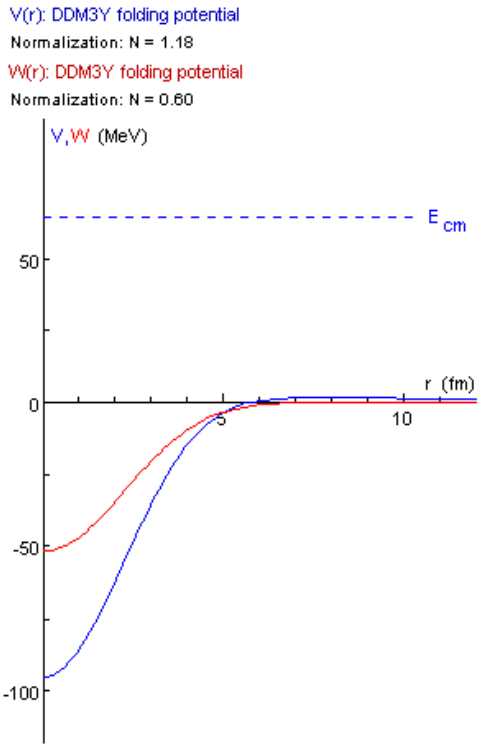

Figure 6: Optical potential of $d + {}^{24}Mg$ at $E_{lab} = 70$ MeV.

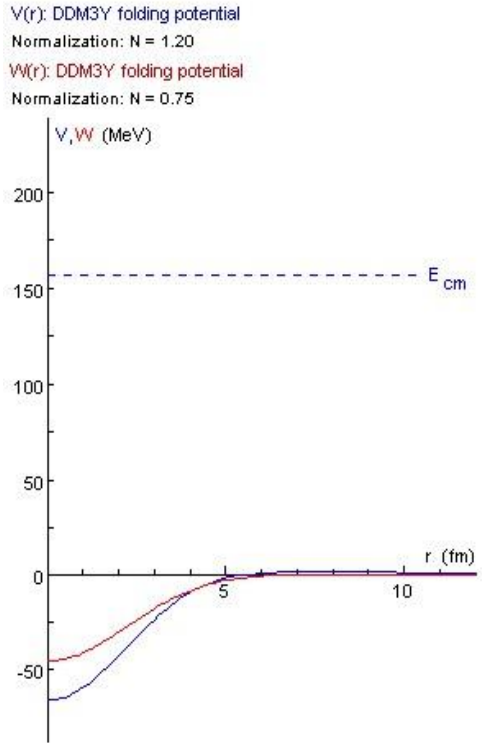

Figure 7: Optical potential of $d + {}^{24}Mg$ at $E_{lab} = 68$ MeV.

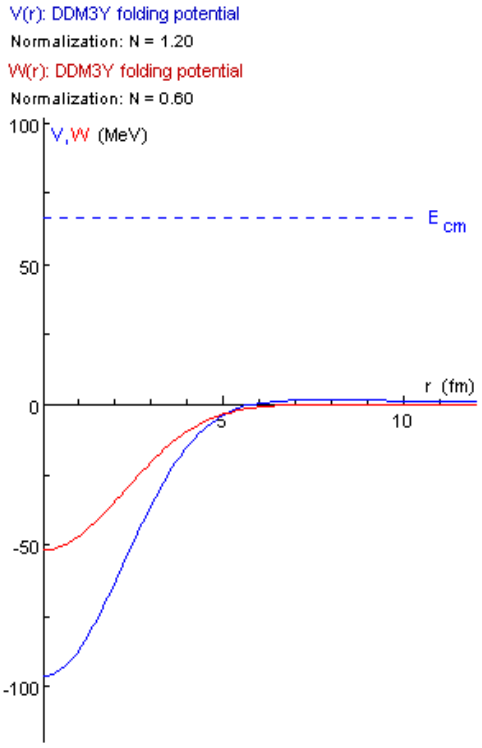

Figure 8: Optical potential of $d + {}^{24}Mg$ at $E_{lab} = 72$ MeV.

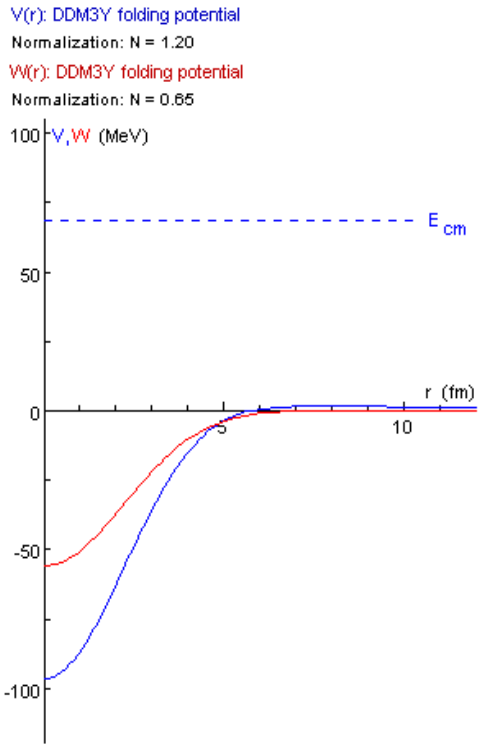

Figure 9: Optical potential of $d + {}^{24}Mg$ at $E_{lab} = 74$ MeV.

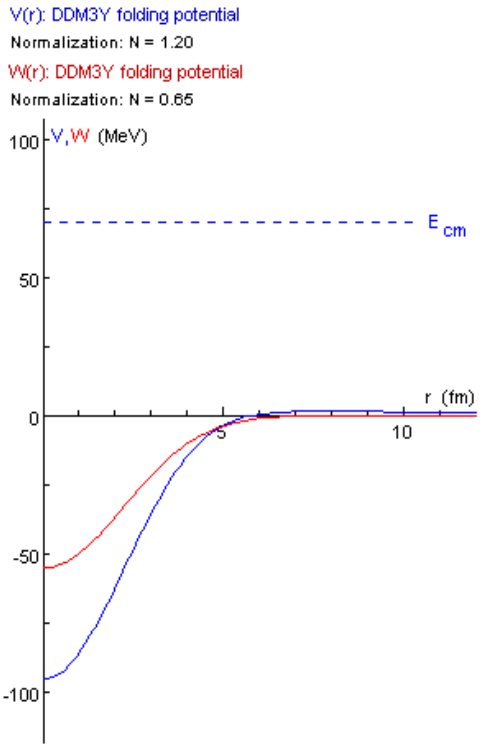

Figure 10: Optical potential of $d + {}^{24}Mg$ at $E_{lab} = 76$ MeV.

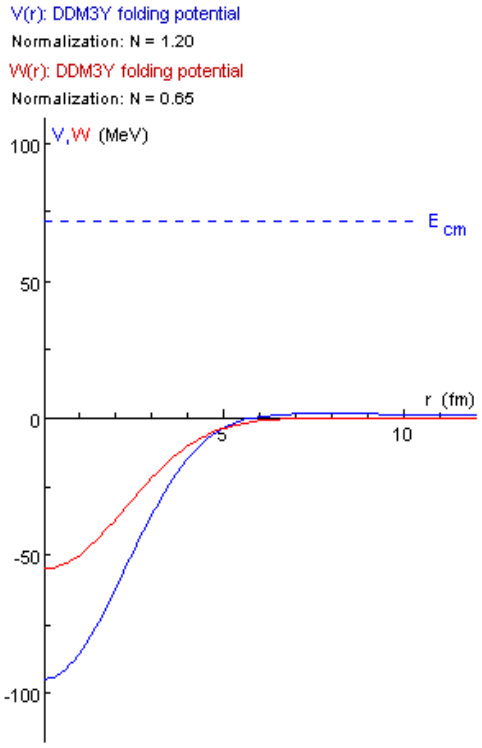

Figure 11: Optical potential of $d + {}^{24}Mg$ at $E_{lab} = 78$ MeV.

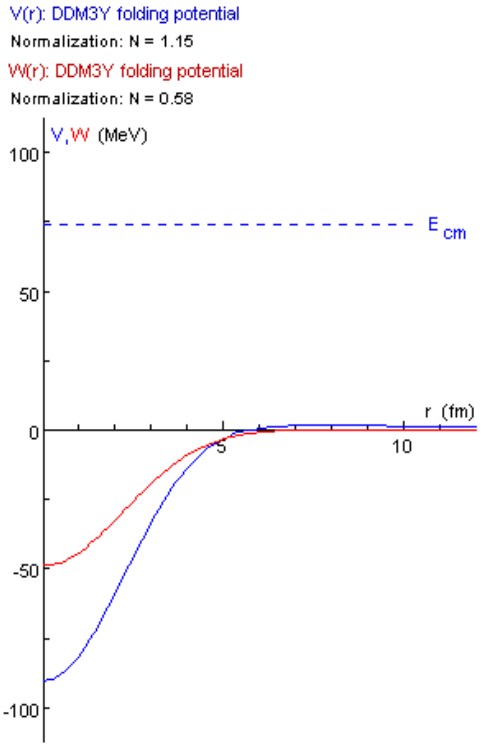

Figure 12: Optical potential of $d + {}^{24}Mg$ at $E_{lab} = 80$ MeV.

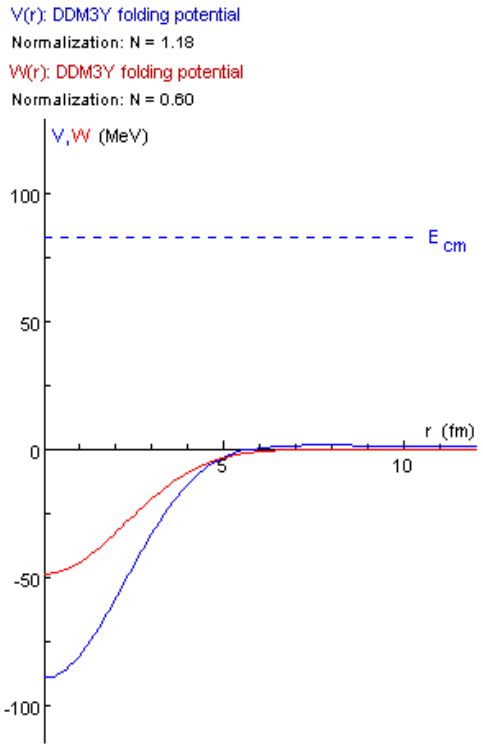

Figure 13: Optical potential of $d + {}^{24}Mg$ at $E_{lab} = 90$ MeV.

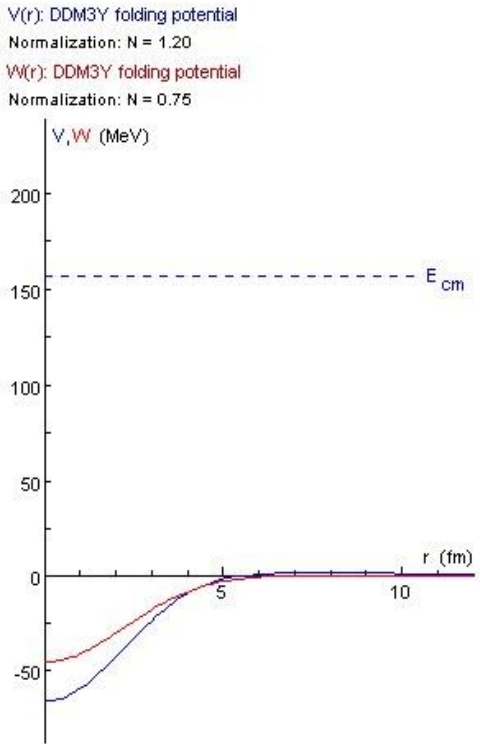

Figure 14: Optical potential of $d + {}^{24}Mg$ at $E_{lab} = 170$ MeV.

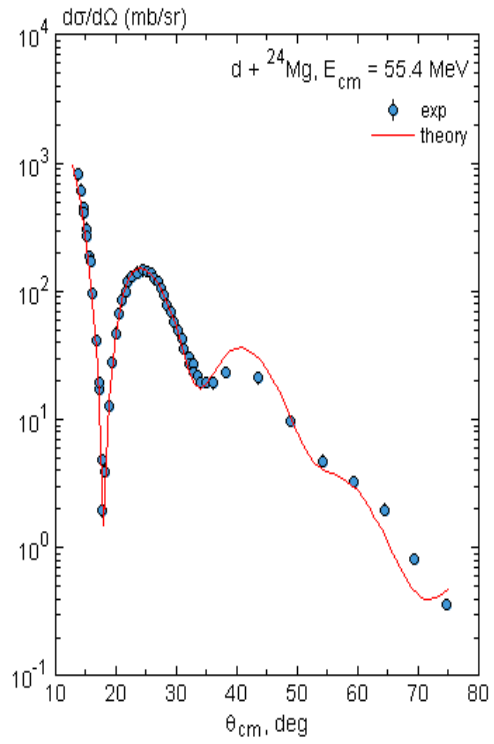

Figure 15: Differential cross-section of $d + {}^{24}Mg$ at $E_{lab} = 60$ MeV.

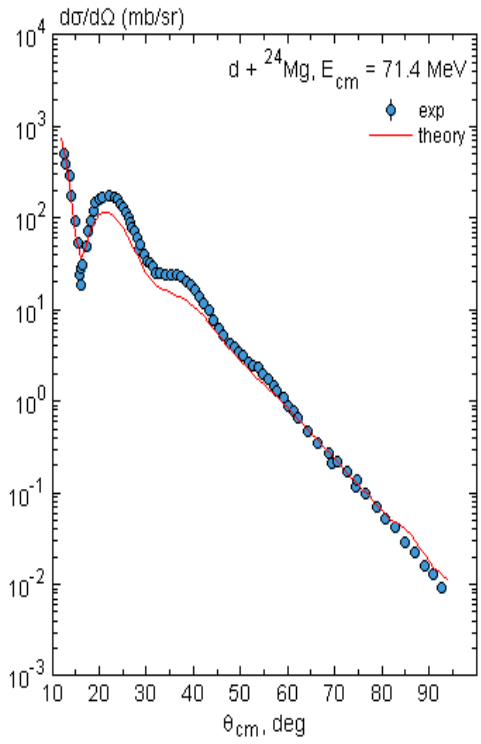

Figure16. Differential cross-section of $d + {}^{24}Mg$ at $E_{lab} = 62$ MeV.

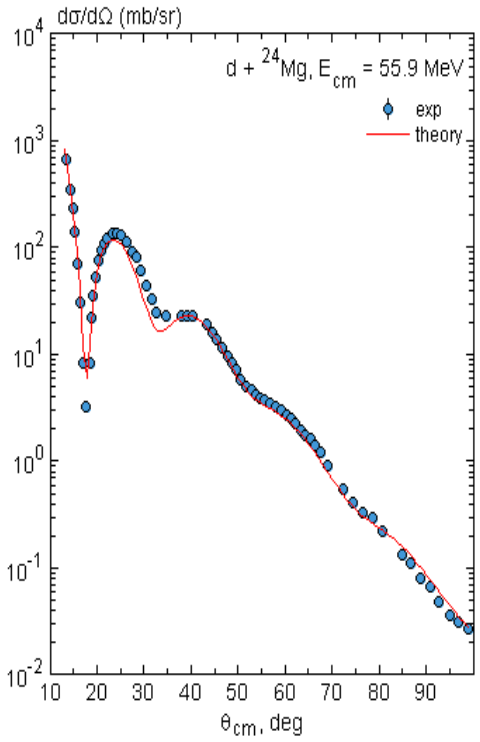

Figure 17: Differential cross-section of $d + {}^{24}Mg$ at $E_{lab} = 60.6$ MeV.

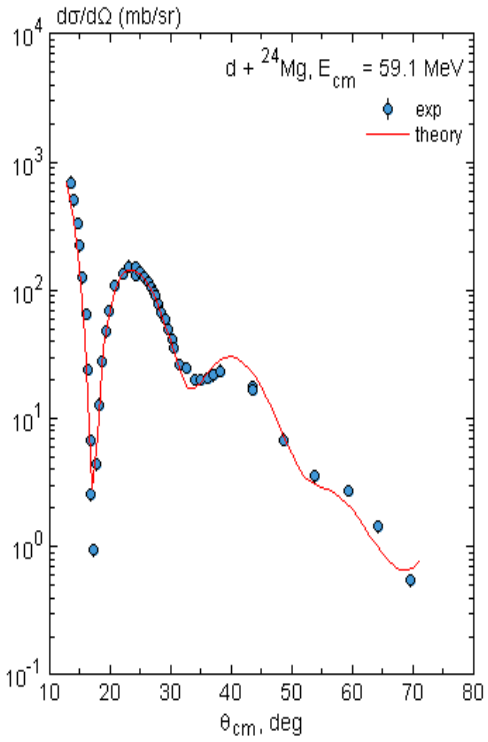

Figure 18: Differential cross-section of $d + {}^{24}Mg$ at $E_{lab} = 64$ MeV.

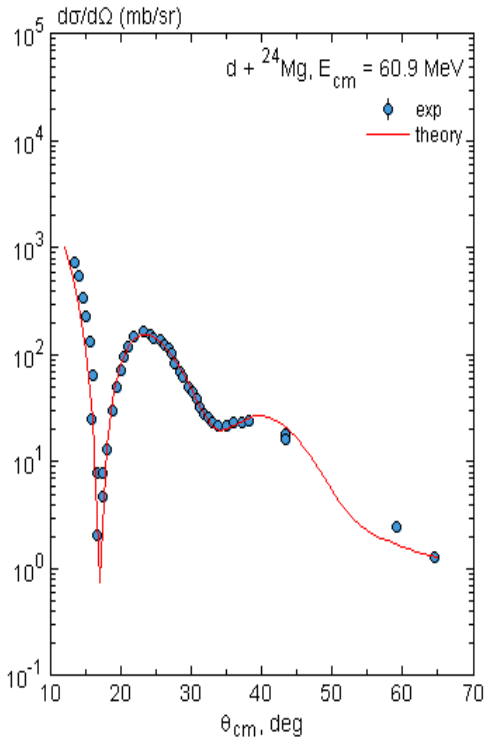

Figure 19: Differential cross-section of $d + {}^{24}Mg$ at $E_{lab} = 66$ MeV.

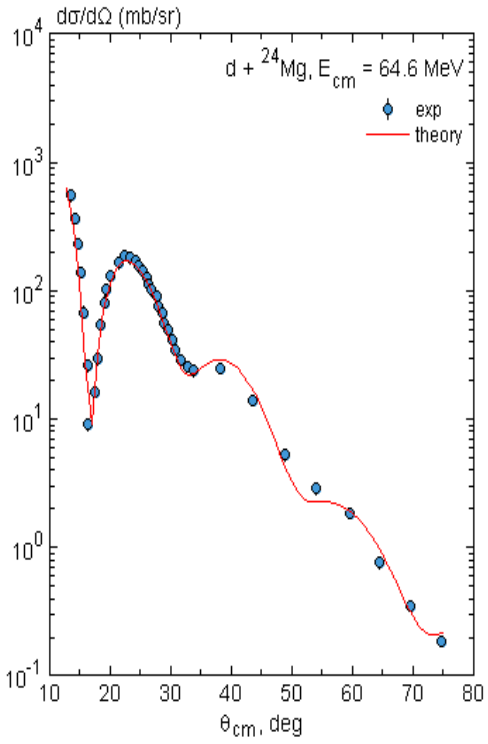

Figure 20: Differential cross-section of $d + {}^{24}Mg$ at $E_{lab} = 70$ MeV.

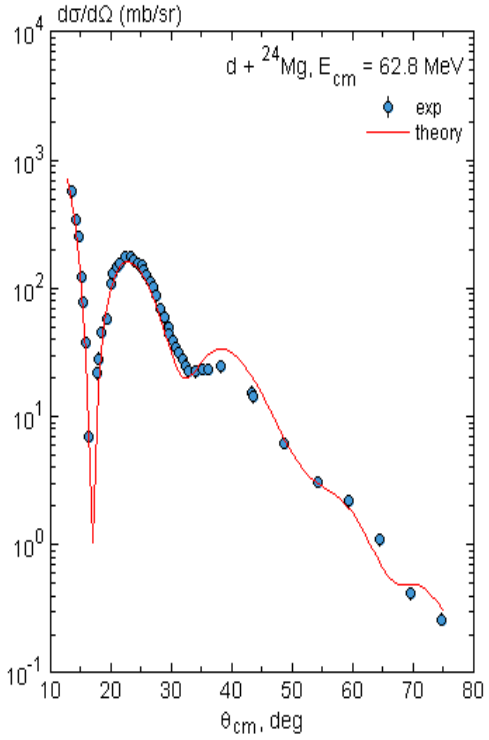

Figure 21: Differential cross-section of $d + {}^{24}Mg$ at $E_{lab} = 68$ MeV.

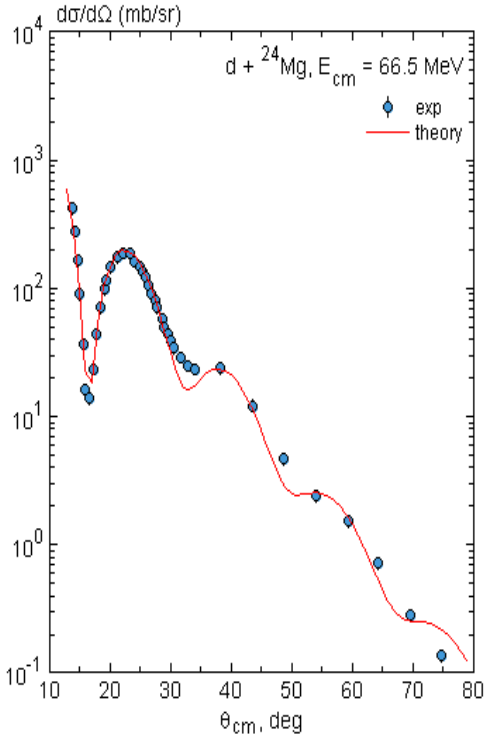

Figure 22: Differential cross-section of $d + {}^{24}Mg$ at $E_{lab} = 72$ MeV.

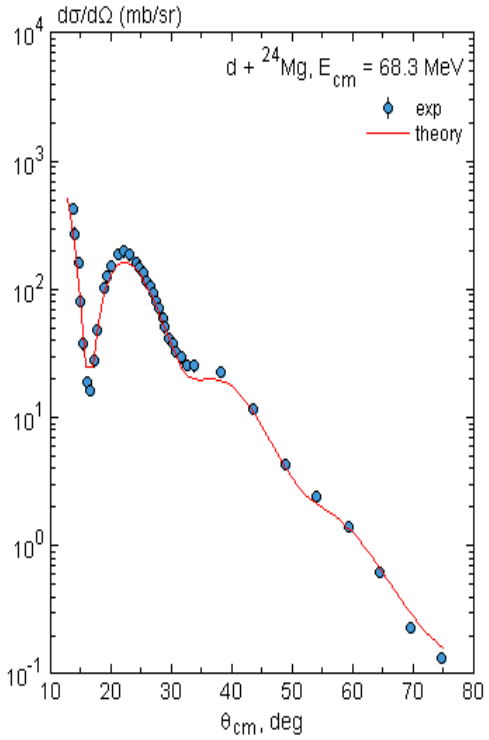

Figure 23: Differential cross-section of $d + {}^{24}Mg$ at $E_{lab} = 74$ MeV.

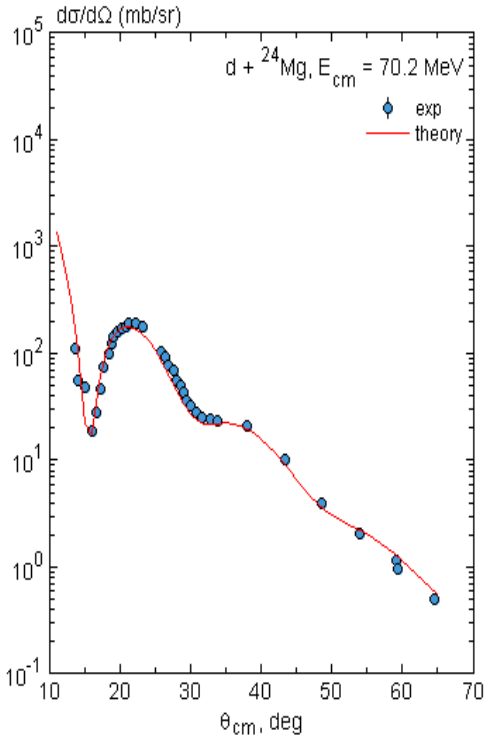

Figure 24: Differential cross-section of $d + {}^{24}Mg$ at $E_{lab} = 76$ MeV.

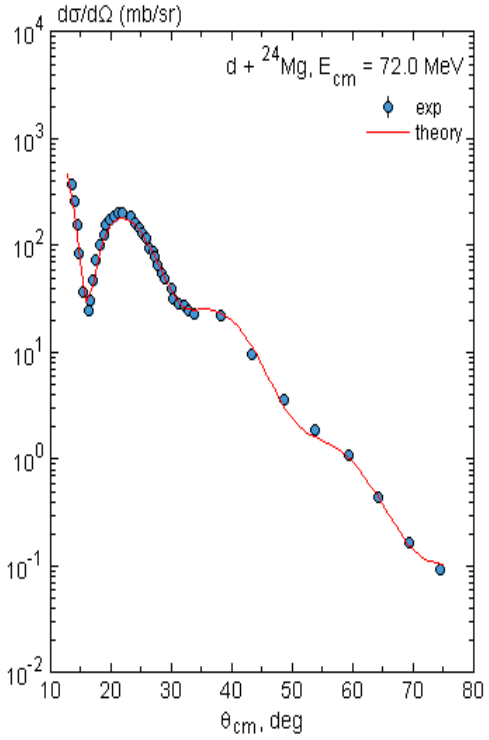

Figure 25: Differential cross-section of $\mathrm{d} + {}^{24}\mathrm{Mg}$ at $\mathrm{E_{lab}} = 78$ MeV.

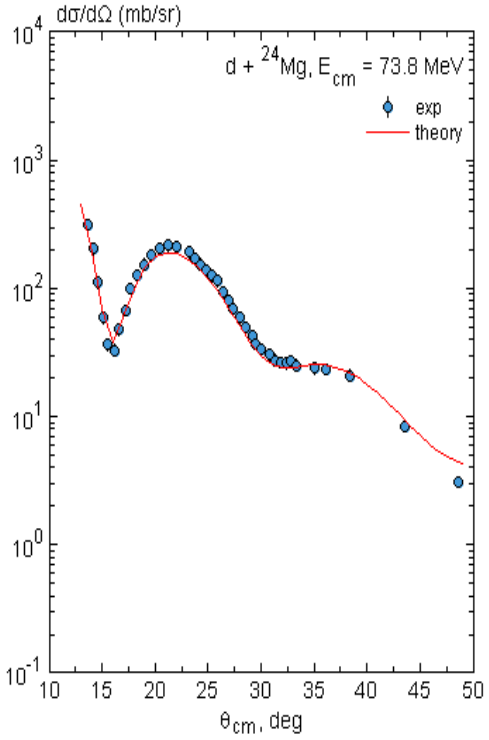

Figure 26: Differential cross-section of $\mathrm{d} + {}^{24}\mathrm{Mg}$ at $\mathrm{E_{lab}} = 80$ MeV.

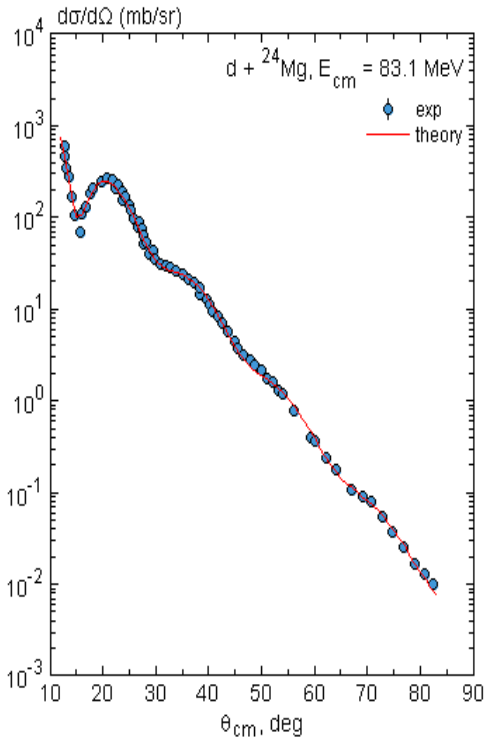

Figure 27: Differential cross-section of $\mathrm{d} + {}^{24}\mathrm{Mg}$ at $\mathrm{E_{lab}} = 90$ MeV.

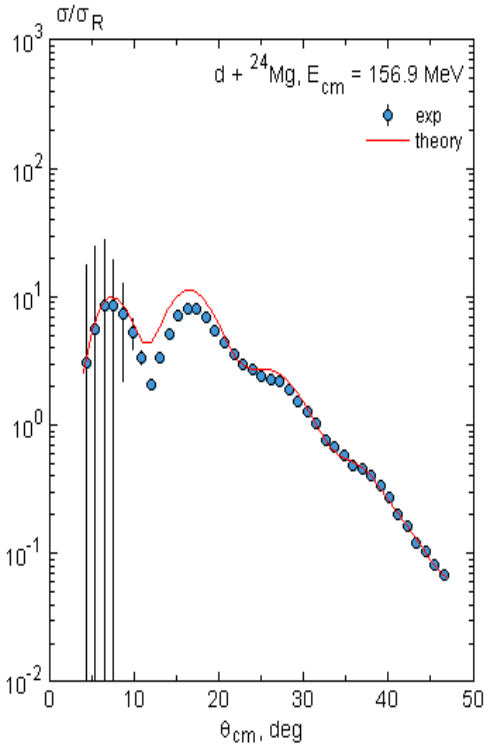

Figure 28: Differential cross-section of $\mathrm{d} + {}^{24}\mathrm{Mg}$ at $\mathrm{E_{lab}} = 170$ MeV.

The folded potentials of the elastically scattered deuteron from $^{24}\mathrm{Mg}$ at various incident energies were determined. The optical potential components were assumed to be identical, except for the differing renormalization factors $N_{r(i)}$. The renormalization process adjusted the strengths of the folded potential to match experimental findings.

Larger renormalization factors, N_r, were required for the real component of the optical potential, while smaller values of N_i, were obtained for the imaginary component of the OP. The radial shape of the strengths of the derived potentials at the various energies were obtained and are shown in Figures 1, 2, 3, 4, 5, 6, 7, 8, 9, 10, 11, 12, 13 &14. These potentials exhibited strong and attractive qualities of the nuclear force within short internuclear distances of around $r\sim 6$ fm. Across all studied interactions, the potentials exhibited a smooth decrease over short distances and took the Woods-Saxon shape. Additionally, the differential cross-sections were computed and compared with experimental data in order to assess the effectiveness of the generated optical potential. Plots of the differential cross-sections as a function of angle in the centre of mass (θ_{cm}) are displayed in Figures 15, 16, 17, 18, 19, 20, 21, 22, 23, 24, 25, 26, 27 & 28. Excellent agreements of differential cross-sections between the experimental data and the current computation were observed at all incident energies. At both small and large angles, the angular distributions showed consistent matches between the computed and experimental values.

CONCLUSION

Double-folding model calculations of $\mathrm{d} + {}^{24}\mathrm{Mg}$ were performed in the elastic channel within the incident laboratory energies of $60 - 170$ MeV. The optical potentials of the density-dependent B3Y-Fetal interaction were derived by convolving it over the ground state densities of the deuteron and ${}^{24}\mathrm{Mg}$ inside the DFM framework. The derived potentials were attractive and short-ranged over small nuclear distances of about $0 \leq r \leq 6$ fm. The folded potentials were also deeper at smaller internuclear distances of about $r \leq 2$ fm. Based on the potential of the double-folding model, the current optical model analysis successfully reproduced the experimental results. This remarkable agreement demonstrated the suitability and reliability of the double-folding model and the B3Y-Fetal interaction as theoretical tools for understanding nuclear reaction data. A consistent explanation of the scattering data was given using the DFM. The results of the current study should motivate interest in using the present formulation of the OP, B3Y-Fetal interaction, as well as its variations to analyse and study nuclear reactions.

REFERENCES

Abenga, R. C., Fiase, J. O., & Ibeh, G. J. (2020). Optical Model Analysis of $\alpha + {}^{40}\mathrm{Ca}$ at $\mathrm{E_{Lab}}$= 104 and 141.7 MeV Using a Mass-Dependent M3Y-Type Effective Interaction. *Nigerian Annals of Pure and Applied Science*, *3*(2), 252–260.

Abenga, R. C., Ibrahim, Y. Y., & Adamu, I. D. (2023). Double Folding Potential and the Deuteron-Nucleus Inelastic Scattering in the Optical Model Framework. *Open Access Library Journal*, *10*, 1–16. **[Crossref]**

Abenga, R. C., Yahaya, Y. I., & Adamu, I. D. (2021). Double Folding Potential of Deuteron Elastic Scattering on Target Nuclei in the Mass Range of $50 \leq \mathrm{A} \leq 208$ Using a Mass-Dependent Effective Interaction. *Bayero Journal of Physics and Mathematical Sciences*, *01*(13), 1–14.

Amer, H. A., Amar, A., Hamada, S., Bondouk, I. I., & El-Hussiny, F. A. (2016). Optical and Double Folding Model Analysis for Alpha Particles Elastically Scattered from ${}^{9}\mathrm{Be}$ and ${}^{11}\mathrm{B}$ Nuclei at Different Energies. *World Academy of Science, Engineering and Technology, Open Science Index 110, International Journal of Chemical and Molecular Engineering*, *10*(2), 161–166.

Anantaraman, N., Toki, H., & Bertsch, G. F. (1983). An Effective Interaction for Inelastic Scattering Derived from the Paris Potential. *Nuclear Physics, Section A*, *398*(2), 269–278. **[Crossref]**

Bäumer, C., Bassini, R., van den Berg, A. M., De Frenne, D., Frekers, D., Hagemann, M., Hannen, V. M., Harakeh, M. N., Heyse, J., de Huu, M. A., Jacobs, E., Mielke, M., Rakers, S., Schmidt, R., Sohlbach, H., & Wörtche, H. J. (2001). Deuteron Elastic and Inelastic Scattering from ${}^{12}\mathrm{C}$, ${}^{24}\mathrm{Mg}$, and ${}^{58}\mathrm{Ni}$ at 170 MeV. *Physical Review C - Nuclear Physics*, *63*(3), 376011–376014. **[Crossref]**

Behairy, K., Zakaria, M. M., & Hassanain, M. A. (2015). Elastic and Inelastic α -Scatterings from ${}^{58}\mathrm{Ni}$, ${}^{116}\mathrm{Sn}$, and ${}^{208}\mathrm{Pb}$ Targets at 288, 340, 480, and 699 MeV. *Brazilian Journal of Physics*, *54*(5), 1–5. **[Crossref]**

Brandan, M. E., & Satchler, G. R. (1997). The Interaction Between Light Heavy-Ions and What it Tells Us. *Physics Reports*, *285*, 143–243.

Burtebayev, N., Janseitov, D. M., Kerimkulov, Z., Alimov, D., Nassurlla, M., Valiolda, D. S., Mauyey, B., Demyanova, A. S., Hamada, S., & Aimaganbetov, A. (2020). Elastic and Inelastic Scattering of Deuterons from ${}^{13}\mathrm{C}$. *Journal of Physics: Conference Series*, *1555*, 1–7. **[Crossref]**

De Vries, H., De Jager, C. W., & De Vries, C. (1987). Nuclear Charge-Density-Distribution Parameters from Elastic Electron Scattering. *Atomic Data and Nuclear Data Tables*, *36*(3), 495–536.

El-Attar, A. L., Farid, M. E., & El-Aref, M. G. (2008). Optical Model Analyses of Deuteron Inelastic Scattering. *9th International Conference for Nuclear Sciences and Applications, Sharm Al Sheikh (Egypt)*, 1239.

Farid, M. E. (2002). Heavy Ion Double Folding Cluster Optical Potentials. *Physical Review C*, *65*(June), 11–13. **[Crossref]**

Farid, M. E., Alsagheer, L., Alharbi, W. R., & Ibraheem, A. A. (2014). Analysis of Deuteron Elastic Scattering in the Framework of the Double Folding Optical Potential Model. *Life Science Journal*, *11*(5), 208–216. **[Crossref]**

Farid, M. E., Mahmoud, Z. M. M., & Hassan, G. S. (2001). Analysis of Heavy Ions Elastic Scattering Using

the Double Folding Cluster Model. *Nuclear Physics A*, *691*, 671–690.

Fiase, J. O., Devan, K. R. S., & Hosaka, A. (2002). Mass Dependence of M3Y-Type Interactions and the Effects of Tensor Correlations. *Physical Review C - Nuclear Physics*, *66*(1), 014004–014010. **[Crossref]**

Hagino, K., Takehi, T., & Takigawa, N. (2006). No-Recoil Approximation To The Knock-On Exchange Potential in the Double Folding Model for Heavy-Ion Collisions. *Physical Review C - Nuclear Physics*, *74*(3), 2–5. **[Crossref]**

Hamada, S., Bondok, I., & Abdelmoatmed, M. (2016). Double Folding Potential of Different Interaction Models for $^{16}O + ^{12}C$ Elastic Scattering. *Brazilian Journal of Physics*, 1–6. **[Crossref]**

Ibraheem, A. A. (2016). Analysis of Deuteron-Nucleus Scattering Using Sao Paulo Potential. *Brazilian Journal of Physics*, *46*(6), 746–753. **[Crossref]**

Ibraheem, A. A., Branch, A., Farid, M. E., & Elshamy, E. F. (2023). Comprehensive Examination of the Elastic Scattering Angular Distributions of $^{10}C + ^{4}He$, ^{27}Al, ^{58}Ni, and ^{208}Pb Using Various Potentials. *Revista Mexicana Defisica*, *69*(June), 1–13.

Khoa, D. T., & Von Oertzen, W. (1993). A Nuclear Matter Study Using the Density-Dependent M3Y Interaction. *Physics Letters B*, *304*(12), 8–16. **[Crossref]**

Khoa, D. T., Von Oertzen, W., & Ogloblin, A. A. (1996). Study of the Equation of State for Asymmetric Nuclear Matter and Interaction Potential Between Neutron-Rich Nuclei Using the Density-Dependent M3Y Interaction. *Nuclear Physics A*, *602*, 98–132. **[Crossref]**

Kobos, A. M., Brown, B. A., Hodgson, P. E., Satchler, G. R., & Budzanowski, A. (1982). Folding Model Analysis of α-Particle Elastic Scattering with a Semirealistic Density-Dependent Effective Interaction. *Nuclear Physics, Section A*, *384*(1–2), 65–87. **[Crossref]**

Kurkcuoglu, M. E., Aytekin, H., & Boztosun, I. (2006). An Investigation of the $^{16}O + ^{16}O$ Elastic Scattering by Using Alpha-Alpha Double Folding Potential in Optical Model Formalism. *Modern Physics Letters A*, *21*(29), 2217–2232.

Love, W. G., & Owen, L. W. (1975). Exchange Effects from Realistic Interactions in the Reformulated Optical Model. *Nuclear Physics A*, *239*, 74–82. **[Crossref]**

Moharram, S. A., & El-Shal, A. O. (2002). Spin Polarized Cold and Hot Dense Neutron Matter. *Turk Journal of Physics*, *26*, 167–177.

Olorunfunmi, S. D., & Olatinwo, A. S. (2023). Analysis of Elastic Scattering Cross Sections of ^{16}O on ^{27}Al and ^{154}Sm Using the Semi-Microscopic Double Folding Model. *Ife Journal of Science*, *25*(2), 239–250.

Satchler, G. R. (1983). *Direct Nuclear Reactions*. Oxford University Press.

Satchler, G. R., & Love, W. G. (1979). Folding Model Potentials from Realistic Interactions for Heavy-Ion Scattering. *Physics Reports (Review Section of Physics Letters)*, *55*(3), 183–254. **[Crossref]**

Zang, G.-L., Zang, H.-Q., Liu, Z.-H., Zang, C.-L., Lin, C.-J., Yang, F., An, G.-P., Jia, H.-M., Wu, Z.-D., Xu, X.-X., Bai-Chun-Lin, & Yu, N. (2007). Double Folding Model Calculation Applied to the Real Part of Interaction Potential. *High Energy Physics and Nuclear Physics*, *13*(7), 634–641. **[Crossref]**